ADVANCED MATERIALS INTERFACES

Supporting Information

for *Adv. Mater. Interfaces,* DOI: 10.1002/admi.201400227

Strongly Coupled Interfaces between a Heterogeneous Carbon Host and a Sulfur-Containing Guest for Highly Stable Lithium-Sulfur Batteries: Mechanistic Insight into Capacity Degradation

Hong-Jie Peng, Ting-Zheng Hou, Qiang Zhang, Jia-Qi Huang, Xin-Bing Cheng, Meng-Qing Guo, Zhe Yuan, Lian-Yuan He, and Fei Wei*

Supporting Information for

Strongly Coupled Interfaces between Heterogeneous Carbon Host and Sulfur-Containing Guest for Highly-Stable Lithium-Sulfur Batteries: Mechanistic Insight into Capacity Degradation

Hong-Jie Peng, Ting-Zheng Hou, Qiang Zhang, Jia-Qi Huang, Xin-Bing Cheng, Meng-Qing Guo, Zhe Yuan, Lian-Yuan He, Fei Wei*

H. J. Peng, T. Z. Hou, Prof. Q. Zhang, Dr. J. Q. Huang, X. B. Cheng, M. Q. Guo, Z. Yuan, L. Y. He, Prof. F. Wei
Beijing Key Laboratory of Green Chemical Reaction Engineering and Technology
Department of Chemical Engineering
Tsinghua University
Beijing 100084, PR China
E-mail: zhang-qiang@mails.tsinghua.edu.cn (Q. Zhang)

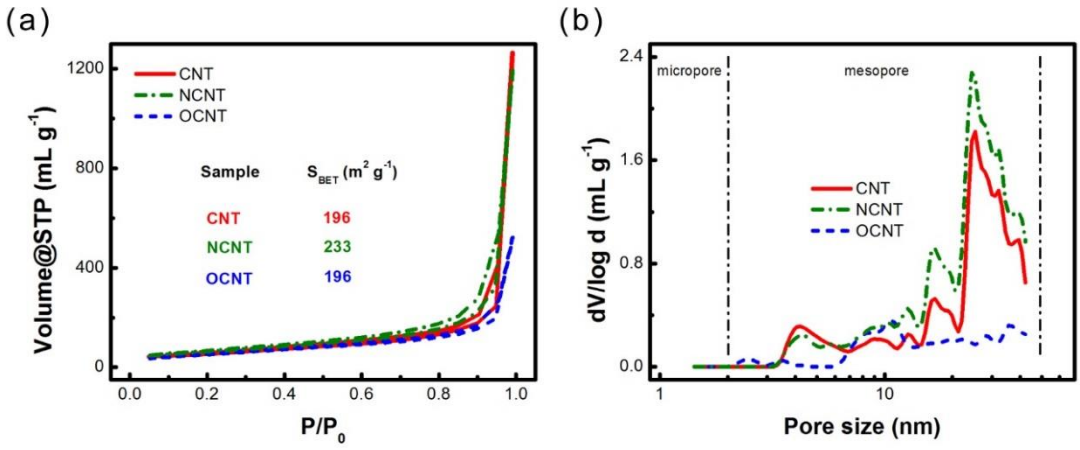

Figure S1. (a) N_2 sorption isotherm, BET specific surface area, and (b) pore size distribution based on QSDFT model of CNTs, NCNTs, and OCNTs.

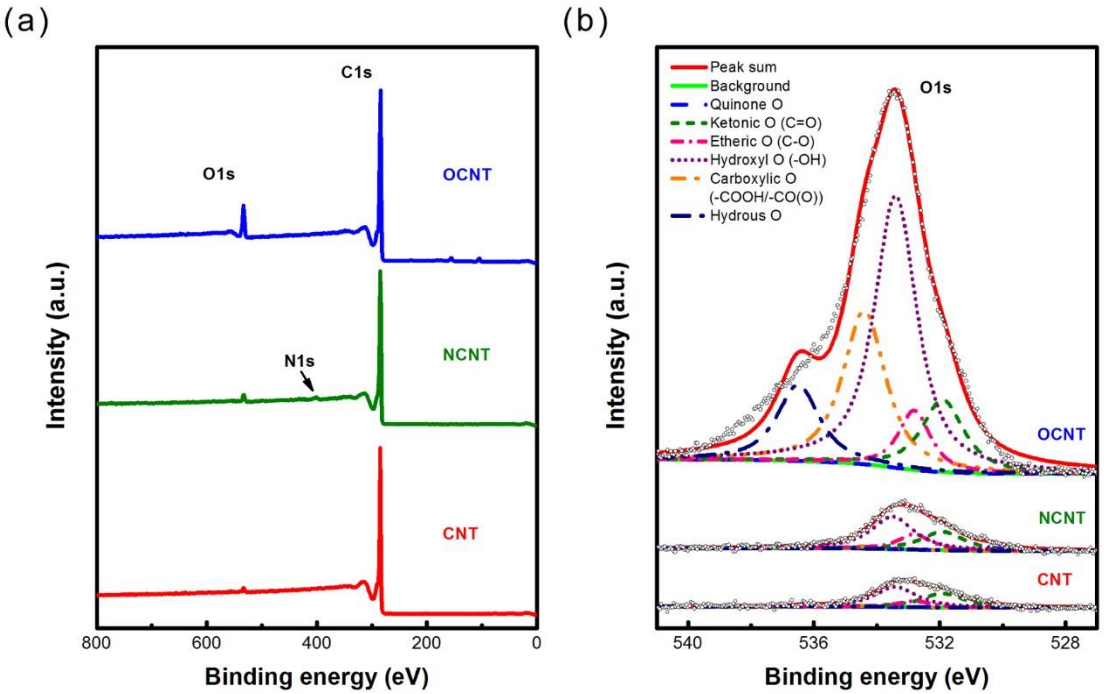

Figure S2. The XPS spectra of (a) survey scans and (b) O1s region of CNTs, NCNTs, and OCNTs.

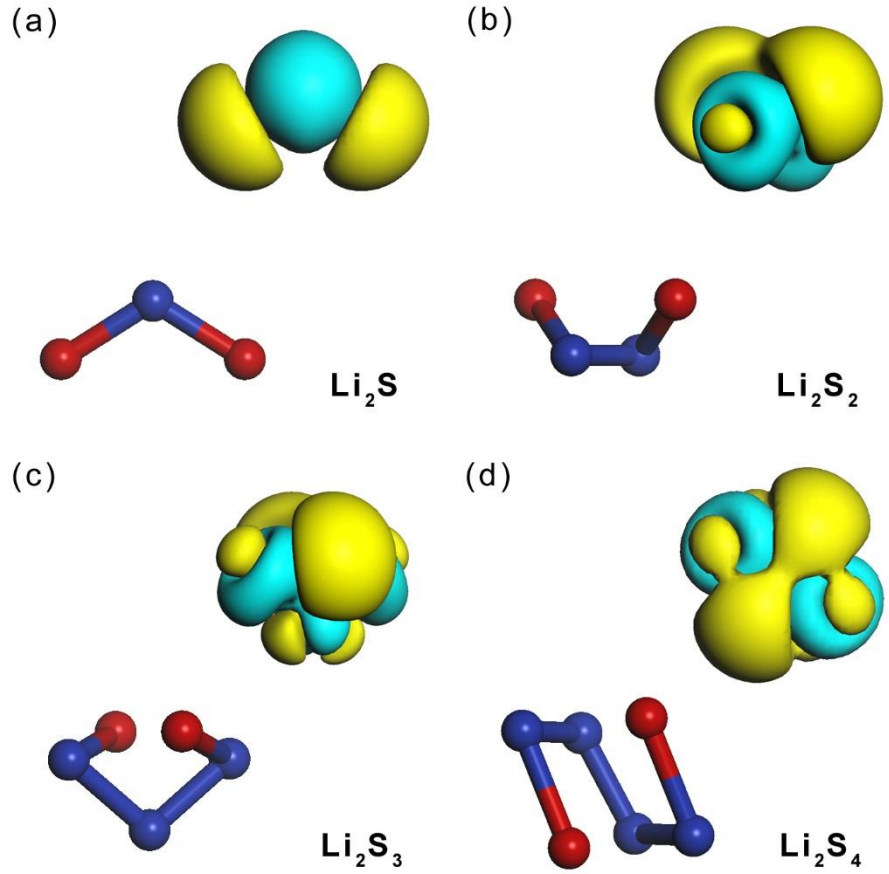

Figure S3. First-principle calculation of polar (a) Li_2S, (b) Li_2S_2, (c) Li_2S_3, and (d) Li_2S_4, showing the optimized molecular configuration and corresponding deformation charge density. In molecular configuration, the lithium and sulfur atoms are denoted as spheres in red and blue respectively; while in distribution of deformation charge density, donation/acceptance of electron is denoted as light yellow/cyan respectively.

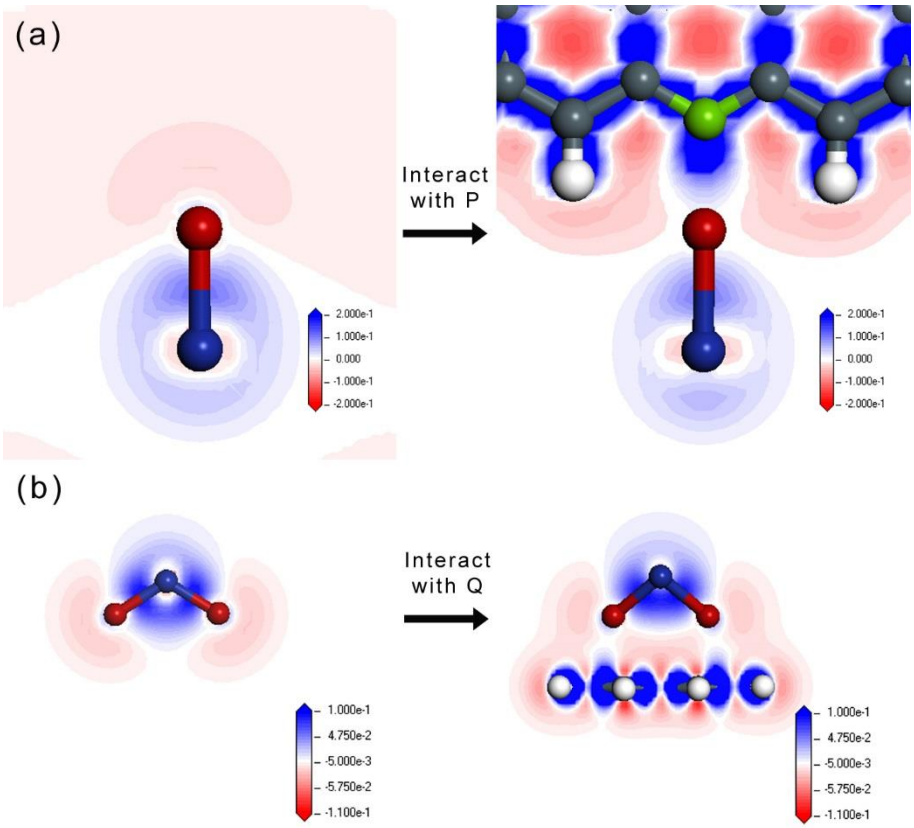

Figure S4. First-principle calculation of deformation charge distribution at the Li_2S adsorption sites of molecule (a) P (top view) and (b) Q (front view), in which the lithium and sulfur atoms are denoted as spheres in red and blue respectively; while increase/decrease of local electron density is denoted as blue/red respectively.

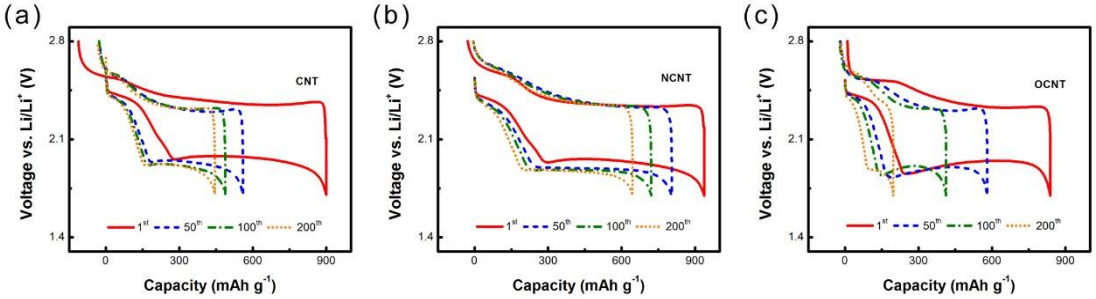

Figure S5. Galvanostatic charge-discharge curves of (a) CNT, (b) NCNT, and (c) OCNT based composite cathode during cycling at current density of 1.0 C.

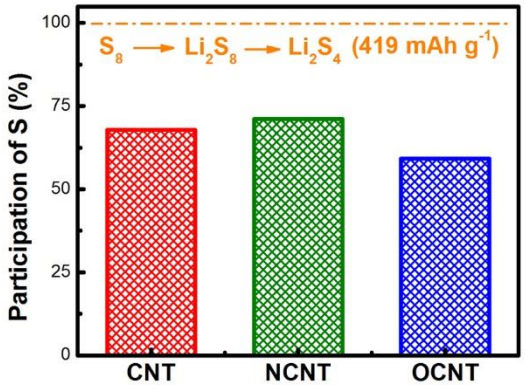

Figure S6. Initial participation of S in CNT, NCNT, and OCNT based composite cathode.

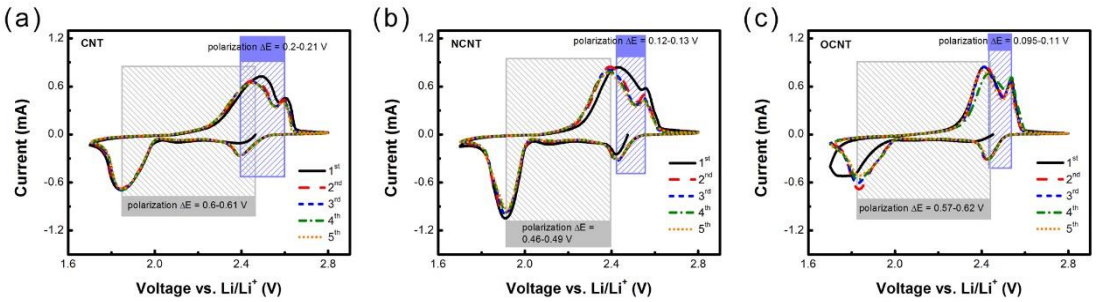

Figure S7. CV profiles of (a) CNT, (b) NCNT, and (c) OCNT based composite cathode at scan rate of 0.1 mV s^{-1}.

Table S1. Summary of nitrogen species in NCNTs.

Sample	Total content of nitrogen (at %)	Relative amounts of nitrogen species (at %)				
		Pyridinic nitrogen (398.4 eV)	Pyrrolic nitrogen (400.1 eV)	Quaternary nitrogen (401.2 eV)	Oxidized nitrogen (402.9 eV)	Chemisorbed nitrogen (404.8 eV)
NCNT	1.76	23.8	2.4	35.3	3.3	35.2

Table S2. Summary of oxygen species in CNTs, NCNTs, and OCNTs.

Sample	Total content of oxygen (at %)	Relative amounts of oxygen species (at %)					
		Quinone oxygen (530.4 eV)	Ketonic oxygen (531.9 eV)	Etheric oxygen (532.8 eV)	Hydroxylic oxygen (533.4 eV)	Carboxylic oxygen (534.4 eV)	Hydrous oxygen (536.5 eV)
CNT	1.40	1.3	34.5	11.6	49.3	2.1	1.2
NCNT	2.09	3.7	27.7	17.4	48.4	2.8	0.0
OCNT	8.88	0.0	11.8	7.2	43.9	24.8	12.3

Table S3. Summary of binding energy between carbon surfaces (P, Q, and C) and S-containing guests (S, Li_2S_4, Li_2S_3, Li_2S_2, and Li_2S) based on first-principle calculation.

	Binding energy (eV)		
	P	Q	C
S	-2.74	-3.13	-2.71
Li_2S	-1.42	-1.12	-1.02
Li_2S_2	-1.24	-1.01	-0.86
Li_2S_3	-1.13	-0.75	-0.62
Li_2S_4	-1.04	-0.73	-0.55